Adsorption characterisation of different volatile organic compounds over alumina, zeolites and activated carbon using inverse gas chromatography

Eva Díaz, Salvador Ordóñez*, Aurelio Vega, José Coca

Department of Chemical Engineering and Environmental Technology, University of Oviedo, Julián Clavería s/n, 33006 Oviedo, Spain

Abstract

Adsorption parameters (enthalpy of adsorption, free energy of adsorption) of several alkanes, cyclic hydrocarbons, aromatic hydrocarbons and chlorinated compounds on different adsorbents (alumina, zeolites 13X and 5 A, and activated carbon) were determined by inverse gas chromatography. Dispersive surface energy interaction and specific interaction parameters were determined for each solute–adsorbent system. It was found that mesoporous alumina presents lower enthalpy of adsorption than the microporous materials. Furthermore, zeolite 13X, which has wider pores than zeolite 5 A, exhibits a higher adsorption capacity.
© 2004 Elsevier B.V. All rights reserved.

Keywords: Inverse gas chromatography; Zeolites; Activated carbon; Alumina; Adsorption

1. Introduction

Volatile organic compounds (VOCs) are among the key pollutants emitted into the atmosphere that cause outdoor air pollution. They are organic compounds that may undergo photochemical reactions with nitrogen oxides in the presence of sunlight, yielding even more hazardous compounds. Photochemical smog and ozone depletion in the stratosphere are results of VOCs activity.

One of the challenges of the Clean Air Act Amendments (CAAA) is the search for efficient and economical VOCs control strategies. Reduction of VOCs concentration to desirable levels can be accomplished by destructive and non-destructive methods. Destructive methods involve oxidation reactions of VOCs to yield non-hazardous chemical species. Non-destructive methods are of physical nature and include adsorption, absorption, condensation and membrane separations (usually pervaporation).

In the adsorption process, VOCs molecules are retained by a solid adsorbent as a result of intermolecular forces. It is used for effluents from vents and storage tanks, although it can also be used in connection with other emission sources. To extend the lifetime of the adsorbent, VOCs are readily desorbed without a change in chemical composition and recovered for reuse or disposal. Activated carbon, silica gel, alumina and zeolitic materials are the most common adsorbents for VOCs abatement.

Granular-activated carbon is the most common type of carbon adsorbent because of its large surface area and efficient VOCs recovery. Studies of adsorption of alkanes on graphite powders and carbon blacks have been reported [1]. Alumina has been employed in adsorptive processes such as temperature swing adsorption (TSA) and pressure swing adsorption (PSA), mainly to pretreat air streams [2]. Adsorption of hydrocarbons on γ-Al$_2$O$_3$ has been extensively reported [3–7].

Zeolites have attracted a great interest due to their catalytic and exchange properties, furthermore they are emerging as versatile alternative adsorbents. Molecular sieve zeolites such

* Corresponding author. Tel.: +34 985 103437; fax: +34 985 103434.
E-mail address: sog@genio.quimica.uniovi.es (S. Ordóñez).

as 13X zeolite (also known as NaX) have been used for hydrocarbon adsorption [8,9], and more recently, molecular sieves of 5 A type (CaA) were also proposed [10,11]. In spite of this, there are not systematic studies comparing the performances of activated carbons, alumina and zeolites for the adsorption of VOCs.

Gas–solid chromatography has been used for many years to study adsorption and catalytic reactions with some advantages with respect to static methods. When its goal is the characterization of the stationary phase, instead of the separation of solutes in the mobile phase, the technique is known as inverse gas chromatography (IGC). IGC measurements can provide information on thermodynamic, surface energy, reaction kinetics, and textural parameters (such as surface area and porosity). IGC has been widely utilized to study synthetic and biological polymers, copolymers, polymer blends, adsorbents [12,13], foods [14], carbon blacks [15] and fibers [16].

In the present work, IGC is used to study thermodynamics of adsorption of several groups of VOCs: hydrocarbons (pentane, hexane, heptane and octane), cyclic compounds (cyclohexene and cycloheptane), aromatic compounds (benzene) and chlorinated compounds (chloroform, trichloroethylene and tetrachloroethylene) on four adsorbents: alumina, activated carbon and molecular sieves 13X and 5 A. Furthermore, the influence of the adsorption on the external surface, as well as the diffusion of molecules within the bulk of material and the surface acidity on adsorption parameters are also reported. The objective of this study was to determine the basic thermodynamic parameters for the adsorption of different kinds of VOCs over different types of adsorbents. Moreover, these parameters have been correlated with the properties of these compounds, as well as with the physico-chemical properties of the solids.

Furthermore, each group of VOCs, depending on their exact structure and on the functional groups present, can show a specific interaction on a given adsorbent. These parameters have two distinct uses: some of them, such as ΔH_{ads} are needed in the design of adsorption units, whereas the more specific parameters are useful predicting the performance of these adsorbents in the adsorption of other compounds, as well as gaining a general understanding of the adsorption process.

2. Experimental

2.1. Materials

The adsorbents used were: γ-Al$_2$O$_3$ (BASF), zeolites 13X and 5 A (Alltech) and activated carbon GF 40 (kindly supplied by Norit, The Netherlands). The activated carbon was chemically activated using the phosphoric acid process. Alumina and activated carbon, available in pellets, were crushed and the fraction between 40/60 mesh was selected. Both commercial zeolites were available in the interval 40/60 mesh.

Solutes employed in adsorption studies were pentane, hexane, heptane and octane from Fluka (>99.5% purity), and cyclohexene, cycloheptane, benzene, chloroform, trichloroethylene and tetrachloroethylene from Panreac (>99% purity). Helium (>99.9995% purity) was supplied by Air Liquide.

2.2. Apparatus and procedure

Chromatographic measurements were carried out with a Varian 3800 gas chromatograph with a thermal conductivity detector. The adsorbent was placed into a 30 cm length of Supelco Premium grade 304 stainless steel column, with passivated inner walls and an inside diameter of 5.3 mm (o.d. 1/4 in.). In order to obtain homogeneous packing, the adsorbent (40/60 mesh) was introduced in small quantities, accompanied by mechanical vibration, and the two ends of the column were then plugged with silane-treated glass wool. The adsorbent loading used in this work were 4.3 g of Al$_2$O$_3$, 0.6 g of zeolites 13X and 5 A and 0.3 g of activated carbon. The columns were then stabilized on the GC system at 200 °C overnight under a helium flow rate of 30 mL/min. In order to avoid detector contamination, the outlet of the column was not connected to the detector during this period.

Measurements were carried out in the temperature range of 200–270 °C. Helium was used as carrier gas, and flow rates were measured using a calibrated soap bubble flowmeter. In order to meet the requirement of adsorption at infinite dilution [17], symmetry of the peaks and retention times reproducible, amounts injected were in the range from 0.05 to 0.8 μL. For each measurement, at least three repeated injections were taken, obtaining reproducible results. Air was used as a marker for the retention time correction, and it was used to ensure the absence of dead volume when a new column is placed in the chromatograph. From the evaluated retention time (t_R, min) and flow-rate (F, cm^3/min) of the carrier gas, the retention volume (V_R, cm^3) was calculated. The specific retention volume, V_g (cm^3/g) is given as:

$$V_g = Fj\frac{(t_R - t_M)}{m}\left(\frac{p_0 - p_w}{p_0}\right)\left(\frac{T}{T_{meter}}\right) \quad (1)$$

where t_R is the retention time (min), t_M the retention time of non-adsorbing marker (hold up time), p_0 the outlet column pressure, p_i the inlet pressure, p_w the vapor pressure of water at the flowmeter temperature (Pa), T the column temperature, T_{meter}, the ambient temperature (K), and j the James–Martin compressibility factor defined as:

$$j = \frac{3}{2}\left[\frac{(p_i/p_0)^2 - 1}{(p_i/p_0)^3 - 1}\right] \quad (2)$$

In addition to chromatography, adsorbents were also characterized by other techniques. The surface area of the adsorbents was determined by nitrogen adsorption at −196 °C with the surface analyser, Micromeritics ASAP-2000 instrument, considering a value of 0.164 nm^2 for the cross-section

of the nitrogen molecule. Acidity strength studies were carried out in a Micromeritics TPD-2900 apparatus connected to a Glaslab 300 mass spectrometer. For this purpose, 0.25 g adsorbent sample was saturated in ammonia—stream of 10% NH_3/90% He—at 50 °C during 30 min, and then heated from 50 to 950 °C at 10 °C/min in a stream of pure He with a flow rate of 50 cm^3/min.

3. Results and discussion

3.1. Textural characterization of adsorbents

Surface area and pore volume, obtained from the analysis of the desorption branch of the nitrogen isotherm using the BJH (Barrett–Joyner–Halenda), are represented in Table 1. Specific surface area of alumina is obtained by BET method widely used. However, it presents serious limitations when it is employed to microporous materials characterization, such zeolites and activated carbon. BET method is based on multilayer adsorption, as takes places in mesoporous materials, whereas microporous ones are characterized by monolayer adsorption, so Langmuir method will be more recommendable for zeolites and activated carbon.

Zeolite 5 A differs from the other adsorbents because it has lower volume of mesopores, whereas zeolite 13X has a higher ratio mesopores to micropores. The higher total pore volume observed for activated carbon, if compared with zeolites, corresponds with a narrower pore size distribution and a larger specific surface area, as shown Fig. 1.

3.2. Diffusion of probe molecules in adsorbents

In order to measure specific interactions of adsorbates with surfaces, the contribution of molecules adsorption on the external surface and molecules diffusion within the bulk of material have been discussed in the literature [18,19]. These authors have demonstrated that by changing the carrier gas flow rate, and thus changing the contact time between adsorbate and adsorbent, it is possible to separate the surface adsorption contribution from the total retention data. No apparent variation of the retention volume for the different solutes was detected for alumina and activated carbon when the carrier gas flowrate was varied. Results for zeolite 13X indicate that

Table 1
Specific surface area and pore volume of alumina, zeolites 13X and 5 A and activated carbon

	S (m^2/g)	V (cm^3/g)	
		Mesopores	Micropores
Al_2O_3	209[a]	0.445	–
Zeolite 13X	571[b]	0.165	0.170
Zeolite 5 A	550[b]	0.062	0.176
Activated carbon	1340[b]	0.294	0.174

[a] Specific surface area obtained by BET method.
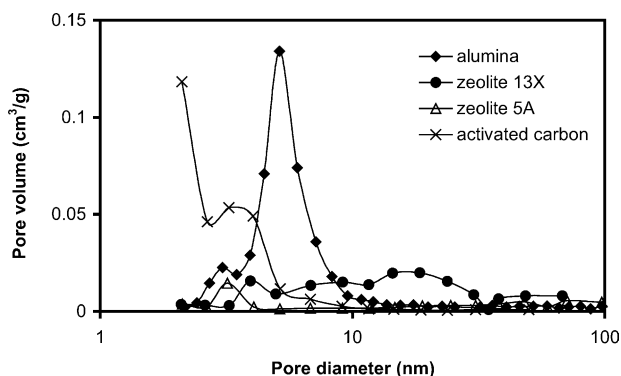[b] Specific surface area obtained by Langmuir method.

Fig. 1. Pore size distribution calculated from nitrogen adsorption isotherms by the BJH method.

specific retention volumes change with carrier gas flowrate at 250 °C for no-aliphatic solutes, as shown in Fig. 2.

For alkanes (C5–C8) no influence in retention volume was observed, neither for zeolite 13X nor zeolite 5 A, this effect was observed for the rest of compounds, especially for aromatic ones (benzene). The increase in retention volume with the decrease of carrier gas flow rate is due to the increasing contribution of molecular diffusion. When the flow rate is high enough and does not affect the retention volume, it is considered that the probe diffusion within the particles is suppressed and the V_g value is the contribution of the surface adsorption of the molecule. Similar results were also obtained by Xie et al. [12] in the case of zeolite NaX, and by Mukhopadhyay and Schreiber [18] and Quin and Schreiber [19] in the case of polymers at higher temperatures than the glass transition.

In order to diffuse through adsorbent particles, the solutes must be adsorbed first on the accessible surface and the more strongly adsorbed molecules have more time for diffusion into the micropores [12]. Since the interaction between the molecules and particle surface is important for internal diffusion, the molecular dimensions and structure of adsorbates are outstanding in diffusional effect in adsorbents. Both from Fig. 2 for zeolite 13X and those for the rest of adsor-
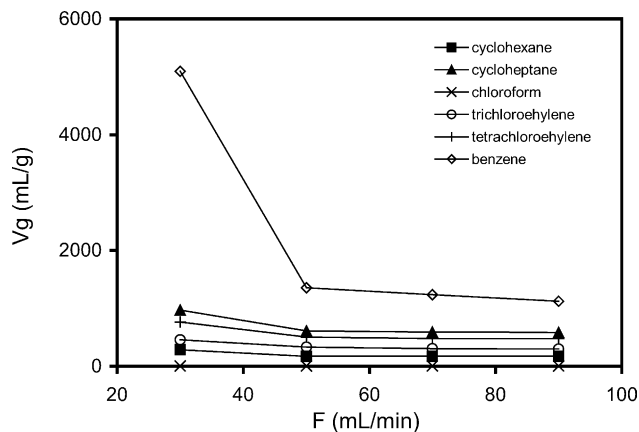

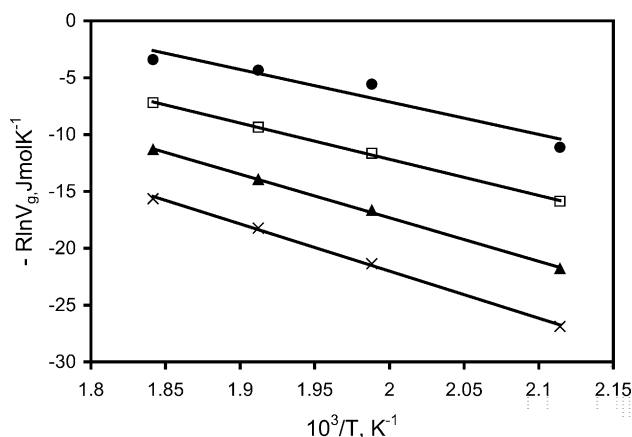Fig. 2. The dependence of specific retention volume with carrier gas flow rate at 250 °C, on zeolite 13X.

Fig. 3. The determination of adsorption enthalpies of probes on alumina: pentane (●), hexane (□), heptane (▲) and octane (×).

bents under study, 50 mL/min was found to be the proper carrier gas flow rate for cyclohexene, cycloheptane, benzene, trichloroethylene and tetraethylene over zeolite 13X, whereas for chloroform and alkanes in the case of the same zeolite 13X and for all the compounds studied for the others adsorbents, at 30 mL/min have reached constant V_g.

3.3. Adsorption parameters

In this study, thermodynamic parameters for adsorption of hydrocarbons (C5–C8), cyclic compounds (cyclohexene and cycloheptane), aromatic compounds (benzene), and chlorinated ones (chloroform, trichloroethylene and tetrachloroethylene) on alumina, activated carbon and molecular sieves 13X and 5 A were determined in the infinite dilution region, in the so-called Henry's law region. These solutes have been chosen in order to analyze the pollutant behaviour in adsorption, as well as the influence of molecular structure in these phenomena.

Thermodynamic data describing the adsorption process were derived from the temperature dependence of the specific retention volume. At low surface coverage, the corresponding enthalpy is given by Eq. (3):

$$\Delta H_{ads} = -R \frac{\partial (\ln V_g)}{\partial (1/T)} \tag{3}$$

Adsorption enthalpies (ΔH_{ads}), were obtained from the slope of plots of $\ln V_g$ versus $1/T$ (Fig. 3), and results are summarized in Table 2.

For all adsorbents the adsorption enthalpy of *n*-alkanes increases with the carbon number. Benzene exhibits more negative ΔH_{ads} than cyclic hydrocarbons and aliphatic and alicyclic hydrocarbons with the same carbon number, i.e. hexane and cyclohexane. High values of ΔH_{ads}, indicate a strong adsorbate–adsorbent interaction, and hence solutes interactions with zeolites and activated carbon were found to be stronger than those on alumina. Similar results were found by Baumgarten et al. [4] and Bravo et al. [5] for the alumina when cyclohexane, benzene and *n*-hexane adsorption was studied. Also, similar results were found by Bilgiç and Aşkin [11] for zeolite 5 A and İnel et al. [9] for zeolite 13X. For chlorinated compounds on zeolites and activated carbon the adsorption enthalpy increases with molecular size, as: chloroform < trichloroethylene < tetrachloroethylene. Alumina, shows a different behavior. Furthermore, it can be seen that the values of ΔH_{ads} are lower (superior in absolute value) to those for heats of liquefaction of these compounds (Table 2). This implies that the enthalpies of adsorption measured are not only due to the heat of condensation of the compounds onto the surface, but also to physico-chemical interactions between solutes and adsorbents, i.e. the adsorbate–adsorbent interactions are preponderant for the initial experimental conditions and that the adsorbate–adsorbate interactions are negligible.

It must be taken into account that accessibility to the microporous network can be assessed by using molecules with similar chemical interaction but with different molecular size. In addition, surface chemistry may be assessed using molecules with different polarity, acid–base properties, etc.; i.e. with different specific interactions with adsorbent surface. Alumina and activated carbon do not possess an ordered crystal structure and consequently the pores are not uniform. Hence, all molecular species, with the possible exception of high-molecular mass polymeric compounds, may enter the pores [11]. The molecular sieves 13X and 5 A have small pores, with uniform free aperture diameter sizes of 0.75 and 0.44 nm, respectively, which are determined by the unit structure of the crystal [23]. In the case of zeolite 13X, solutes can be sorbed into the cavity. Pores of zeolite 5 A cannot be invaded by the studied molecules. These molecules may

Table 2
Adsorption enthalpies (kJ/mol) and solute liquefaction heats for the compounds studied over the different adsorbents

	Alumina	Zeolite 13X	Zeolite 5 A	Activated carbon	ΔH_{liq} (kJ/mol)
Pentane	−28.47	−41.25	−52.96	−48.01	−24.3 [20]
Hexane	−31.81	−49.28	−57.97	−55.43	−27.2 [20]
Heptane	−38.33	−55.19	−63.09	−66.22	−31.7 [20]
Octane	−41.45	−63.62	−69.61	−77.52	−36.6 [20]
Cyclohexane	−33.88	−45.56	−39.71	−48.10	−29.97 [21]
Cycloheptane	−43.45	−52.80	−43.53	−50.64	−38.5 [22]
Benzene	−42.40	−56.92	−58.87	−58.09	−33.92 [21]
Chloroform	−40.56	−49.68	−44.00	−50.61	−31.4 [21]
Trichloroethylene	−34.68	−52.04	−44.84	−51.28	−34.62 [21]
Tetrachloroethylene	−38.59	−53.11	−45.91	−59.35	−34.68 [21]

Table 3
Standard free energy, ΔG_{ads} (kJ/mol), for listed compounds with adsorbents under study at 250 °C

	Alumina	Zeolite 13X	Zeolite 5 A	Activated carbon
Pentane	−3.74	−15.48	−25.93	−15.90
Hexane	−6.35	−20.41	−26.88	−20.90
Heptane	−8.75	−24.57	−32.05	−25.88
Octane	−10.99	−28.85	−37.11	−31.26
Cyclohexane	−5.78	−18.44	−8.23	−19.00
Cycloheptane	−8.90	−23.63	−15.55	−19.43
Benzene	−10.41	−25.78	−27.75	−24.46
Chloroform	−1.17	−19.79	−18.91	−15.34
Trichloroethylene	−8.36	−20.15	−19.83	−18.84
Tetrachloroethylene	−8.90	−22.80	−20.69	−23.21

still be adsorbed on the external surface, which corresponds to the zone of mesoporosity, so values of enthalpy of adsorption are higher for zeolite 13X than for zeolite 5 A. Benzene shows slightly higher values, which can be attributed to the interaction of the π-electrons with the exchangeable cations (sodium in the case of zeolite 13X and calcium in the case of zeolite 5 A). It is remarkable the importance of the shape of pores in the solids: slit-shaped in activated carbons, cylindrical in zeolites and U-shaped in alumina. When studying activated carbons, the minimum dimension of benzene is taken as 0.37 nm, which corresponds to the width of its flat structure; thus, benzene can enter slit-shaped pores wider then 0.37 nm. But it can no go through cylindrical pores with this diameter. In this case, its minimum dimension is taken as 0.57 nm, the distance between two opposite carbon–carbon bonds [23].

From chromatographic data, the standard free energy of adsorption at infinite dilution, ΔG_{ads} (J/mol), can be expressed as [11,24,25]:

$$\Delta G_{ads} = -RT \ln \left[\frac{p_0 V_g}{\pi_0 A} \right] \quad (4)$$

or in an equivalent form [24,26]:

$$\Delta G_{ads} = -RT \ln V_g + C \quad (5)$$

where A is the specific surface area, and π_0 is the spreading pressure of the adsorbed gas in the De Boer standard state, which was taken as 338 μN/m [27]. The parameter, C, is a constant related to the standard states. Data of ΔG_{ads} for the solute–sorbent systems calculated from Eq. (4), at 250 °C, are given in Table 3. The free energy of adsorption for n-alkanes increases with the carbon number and follows the same trend as the adsorption enthalpies.

For a given adsorbate, the free energy of adsorption is the sum of energies of adsorption attributed to dispersive and specific interactions. The standard free energy of adsorption takes into account the standard free energy of adsorption of polar solutes on solid surfaces, namely, the dispersive contribution, ΔG_{ads}^d, and the specific contribution, ΔG_{ads}^s [28]. For n-alkanes $\Delta G_{ads} = \Delta G_{ads}^d$ and changes with the number of carbon atoms in their molecules, the increment of adsorption energy corresponding to methylene group, ΔG_{CH_2}, and
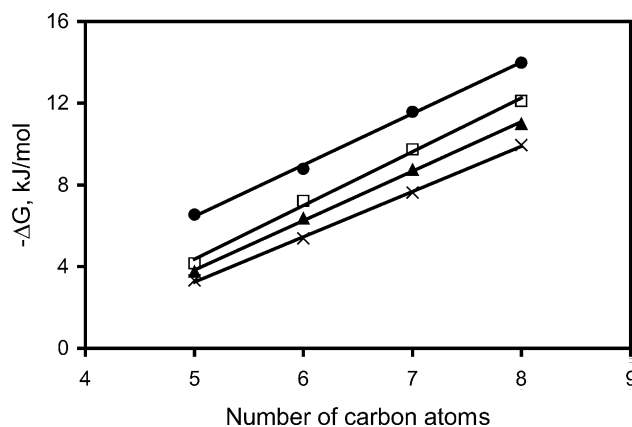

Fig. 4. The free energy of different probe adsorptions on alumina at different temperatures: 200 °C (●), 230 °C (□), 250 °C (▲) and 270 °C (×).

may be calculated from [20]:

$$\Delta G_{CH_2} = -RT \ln \frac{V_{g(n)}}{V_{g(n+1)}} \quad (6)$$

where $V_{g,n}$ and $V_{g,n+1}$ are the specific retention volumes of two consecutive n-alkanes having n and $(n + 1)$ carbon atoms, respectively. ΔG_{CH_2} is independent of the chosen reference state of adsorbed molecule [24]. The slopes of linear functions given in Fig. 4 represent the increment in ΔG_{CH_2}.

As in the case of the free energy of adsorption, the surface free energy of the adsorbent, γ_S (J/m²), may be split into dispersion, γ_S^D, and specific, γ_S^S, contributions, corresponding to the dispersion and specific interactions, respectively [29]:

$$\gamma_S = \gamma_S^S + \gamma_S^D \quad (7)$$

The dispersive component, intrinsic and unspecific for all molecules, is due to London forces and is given by:

$$\gamma_S^D = \frac{1}{4} \frac{\Delta G_{CH_2}^2}{\gamma_{CH_2} N^2 a_{CH_2}^2} \quad (8)$$

where N is the Avogadro number, a_{CH_2} is the area occupied by a $-CH_2$ group (0.06 nm²), and γ_{CH_2} (mJ/m²) is the surface tension of a surface consisting of CH_2 groups, which is a function of temperature (°C):

$$\gamma_{CH_2} = 35.6 + 0.058(20 - T) \quad (9)$$

Table 4 shows γ_S^D values, calculated from Eq. (8); they decrease as temperature increases in all cases. Values of γ_S^D

Table 4
Dispersive component of surface energy, γ_S^D (mJ/m²)

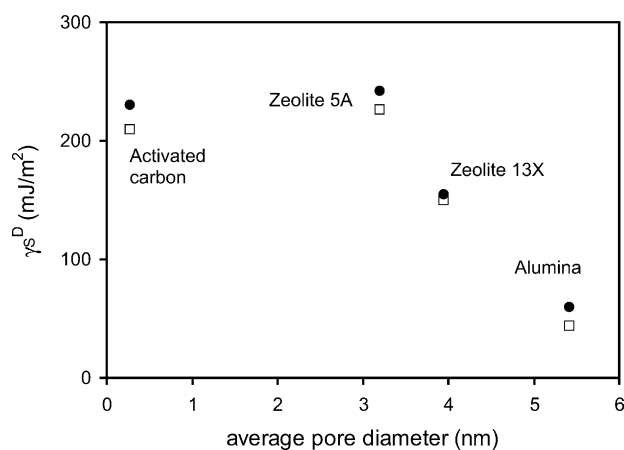| Adsorbent	Alumina	Zeolite 13X	Zeolite 5 A	Activated carbon
200 °C	59.3	154.9	242.0	230.3
230 °C	56.7	153.1	241.1	224.5
250 °C	50.1	152.3	232.6	218.7
270 °C	44.6	150.3	226.9	210.1

Fig. 5. Dependence of γ_S^D (mJ/m^2) on average pore diameter at different temperatures: 200 °C (●) and 270 °C (□).

for zeolites and activated carbon are higher than those obtained for the adsorption of the same compound on polymer surfaces, $\sim$60 mJ/m^2 [25] or compounds such as theophylline and caffeine, $\sim$50 mJ/m^2 [30]. These high values of γ_S^D can be attributed to a high interaction potential in the micropores.

Fig. 5 is a plot of γ_S^D as a function of the average micropores diameter of the adsorbents. It decreases as the average pore diameter increases, which shows the interactions are stronger in the micropores. Several authors have reported the high values of the dispersive component for activated carbons [20,31] and clays [26].

3.4. Specific interaction

In order to get a better understanding of the role of specific adsorption mechanisms, the chromatographic behavior of polar molecules was compared to that of n-alkanes.

The specific component of the surface free energy is closely related with the parameter of specific interaction of polar solutes (I^{sp}). This parameter involves the surface properties in terms of potential and acid–base interactions and may be determined from the difference of free energy of adsorption, $\Delta(\Delta G)$, between a polar solute and the real or hypothetical n-alkane with the same surface area [25] or boiling point, T_b, [32].

$$I^{sp} = \frac{\Delta(\Delta G)}{Na_p} \tag{10}$$

where a_p is the probe surface area. In the present work, a_p is calculated from the liquid density, ρ, and the molar weight of the molecule, M, assuming a spherical molecular shape in a hexagonal close-packed configuration [32].

$$a_p = 1.09 \times 10^{14} \left(\frac{M}{\rho N} \right)^{2/3} \tag{11}$$

The specific interaction parameters, I^{sp}, calculated from Eq. (10), for the four adsorbents, are listed in Table 5. It

Table 5
I^{sp} (mJ/m^2) values determined on alumina, zeolite 13X, zeolite 5 A and activated carbon

Samples	200 °C	230 °C	250 °C	270 °C
Alumina				
Cyclohexane	24.7	16.1	15.5	13.5
Cycloheptane	25.1	20.1	18.9	17.8
Benzene	66.9	63.5	59.5	55.5
Chloroform	16.3	11.5	4.7	0.4
Trichloroethylene	56.2	52.1	49.5	47.8
Tetrachloroethylene	40.8	38.7	36.7	35.3
Zeolite 13X				
Cyclohexane	19.1	18.1	15.5	13.8
Cycloheptane	25.7	24.7	23.1	21.3
Benzene	96.2	93.1	88.8	84.2
Chloroform	24.6	20.3	11.1	5.2
Trichloroethylene	66.6	63.8	61.2	55.4
Tetrachloroethylene	51.6	47.7	45.7	43.3
Zeolite 5 A				
Cyclohexane	89.0	67.3	58.1	52.6
Cycloheptane	107.5	91.2	79.9	37.6
Benzene	135.1	91.6	76.3	52.8
Chloroform	20.7	22.3	15.9	1.1
Trichloroethylene	67.5	54.9	46.9	27.2
Tetrachloroethylene	65.3	62.7	44.9	17.6
Activated carbon				
Cyclohexane	180.1	165.2	156.3	143.1
Cycloheptane	214.8	197.8	188.2	174.9
Benzene	163.9	151.1	141.8	124.9
Chloroform	132.5	121.4	109.3	90.5
Trichloroethylene	162.0	148.4	138.9	122.3
Tetrachloroethylene	148.1	121.8	112.1	105.9

was observed that the temperature affects the specific interaction, this parameter increasing initially and decreasing latter with the increase of temperature. If the interaction is studied according to the family, it is noted that in the case of cyclic hydrocarbons, it does not vary monotonously. Cycloheptane shows higher I^{sp} than cyclohexane with all the adsorbents. Furthermore, I^{sp} is higher for the aromatic ring (benzene) than for cycloalkanes, except with activated carbon as sorbent. For the three chlorinated solutes, I^{sp} depends on size, dipolar moment and polarity of the molecule. Their specific interaction parameters follow the expected trend on the basis of their dipolar moment (1.78 D for trichloroethylene, 1.32 D for tetrachloroethylene and 1.01 D for chloroform) [33], i.e., stronger interaction with increasing polarity.

The trend of the specific interaction parameter I^{sp} with the molecular area of the probe molecules, calculated according to Eq. (11), is depicted in Fig. 6. In a previous work [34], it was observed that the calculation of this parameter based on molecular area was more reliable than if based on boiling points. It is noted that, in general, influence of temperature is not outstanding. Furthermore, there is not a strong influence of temperature on I^{sp} and it does not vary consistently with molecular area, which means that the pores diameter is not the key factor in polar interactions.
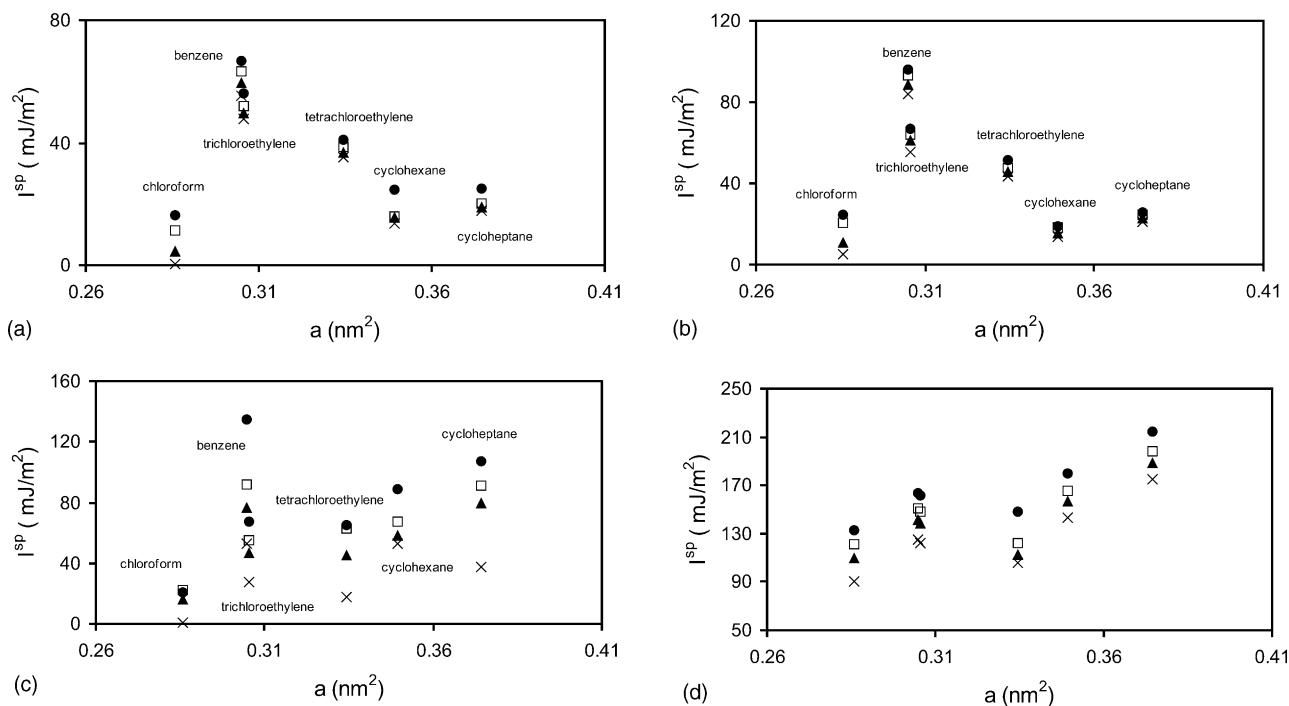
Fig. 6. I^{sp} dependence on area molecules at different temperatures [200 °C (●), 230 °C (□), 250 °C (▲) and 270 °C (×)] for: (a) alumina, (b) zeolite 13X, (c) zeolite 5 A and (d) activated carbon.

3.5. Influence of sorbent acidity on adsorption

Chromatographic data may supply some insight about the influence of sorbent acidity on its adsorption capacity. Alumina, as well as zeolites, has both acid and basic properties. Fig. 7 shows TPD spectra for zeolites 13X and 5 A and alumina.

According to the literature, three kinds of acid sites may be considered, depending on the desorption temperature: weak ($T_D < 250$ °C), medium (250 °C $< T_D < 400$ °C) and strong ($T_D > 400$ °C) acid sites [35]. All the sorbents studied are in the range medium and strong acid sites and zeolites are much more acidic than alumina. This acidity may be correlated with
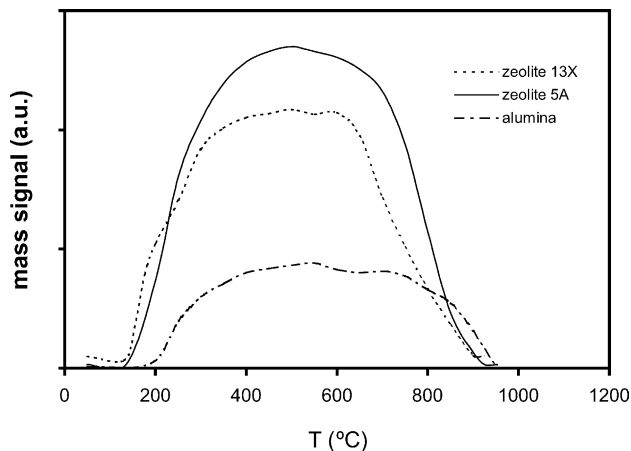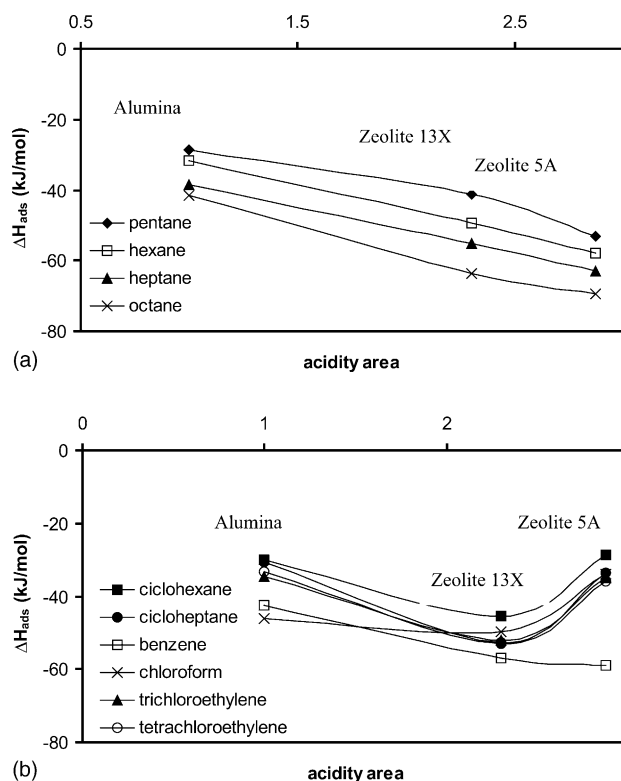

(a)

(b)

Fig. 8. Enthalpies of adsorption dependence of acidity (integration of NH$_3$-TPD) for different compounds: (a) pentane, hexane, heptane and octane; (b) cyclohexane, cycloheptane, benzene, chloroform, trichloroethylene and tetrachloroethylene.

Fig. 7. TPD curve for zeolites 13X and 5 A and alumina, using ammonia as probe molecule.

the adsorption enthalpies, by integration of TPD-curves, as shown in Fig. 8.

It is observed that adsorption enthalpy of *n*-alkanes increases with the increase of the acidity of adsorbent. However, for the other compounds, it was observed a variation of the trend. Adsorption of cyclic and chlorinated compounds is stronger over zeolite 13X than over alumina, but this behaviour is contrary to that which happens over zeolite 5 A. It is noted that both *n*-alkanes and benzene correlate acidity vs. adsorption, whereas it does not happen in the case of cyclic and chlorinated compounds. A possible explanation could be that instead of physico-chemical interaction, steric factors lead the process. This is in agreement with the high difference between cyclohexane–hexane and cycloheptane–heptane. In the case of activated carbon, the solute–adsorbent interaction is different, and probably esteric selectivity of activated carbon is the key, so interaction could be higher.

Acknowledgements

References

[1] E. Papirer, S. Li, H. Balard, J. Jagiello, Carbon 29 (1991) 1135.
[2] S.U. Rege, R.T. Yang, M.A. Buzanowski, Chem. Eng. Sci. 55 (2000) 4827.
[3] M.G. Neumann, J. Chem. Educ. 53 (1976) 708.
[4] E. Baumgarten, F. Weinstrauch, H. Höffkes, J. Chromatogr. 138 (1977) 347.
[5] M. Bravo, A.B. Fuertes, J. Coca, React. Kinet. Catal. Lett. 31 (1986) 173.
[6] F. Thielmann, E. Baumgarten, J. Col. Interf. Sci. 229 (2000) 418.
[7] S. Cai, K. Sohlberg, J. Mol. Catal. 193 (2003) 157.
[8] A.G. Bezus, M. Kocirik, A.V. Kiselev, A.A. Lopatkin, E.A. Vasilyeva, Zeolites 6 (1986) 101.
[9] O. İnel, D. Topaloğlu, A. Aşkin, F. Tümsek, Chem. Eng. J. 88 (2002) 255.
[10] F. Tümsek, O. Inel, Chem. Eng. J. 94 (2003) 57.
[11] C. Bilgiç, A. Aşkin, J. Chromatogr. A 1005 (2003) 281.
[12] J. Xie, M. Bousmina, G. Xu, S. Kaliaguine, J. Mol. Catal. 135 (1998) 187.
[13] M.P. Elizalde-González, R. Ruíz-Palma, J. Chromatogr. A 845 (1999) 373.
[14] A. Boutboul, F. Lenfant, P. Giampaoli, A. Feigenbaum, V. Ducret, J. Chromatogr. A 969 (2002) 9.
[15] E. Papirer, E. Brendle, F. Ozil, H. Balard, Carbon 37 (1999) 1265.
[16] A. Vega, F.V. Díez, P. Hurtado, J. Coca, J. Chromatogr. A 962 (2002) 153.
[17] B. Charmas, R. Leboda, J. Chromatogr. A 886 (2000) 133.
[18] P. Mukhopadhyay, H.P. Schreiber, Macromolecules 26 (1993) 6391.
[19] R.-Y. Quin, H.P. Schreiber, Langmuir 10 (1994) 4153.
[20] C. Herry, M. Baudu, D. Raveau, Carbon 39 (2001) 1879.
[21] V. Majer, V. Svoboda, Enthaphies of Vaporization of Organic Compounds: A Critical Review and Data Compilation, Blackwell Scientific Publications, Oxford, 1985.
[22] H.L. Finke, D.W. Scout, M.E. Gross, J.F. Messerly, G. Waddington, J. Am. Chem. Soc. 78 (1956) 5469.
[23] J. Silvestre-Albero, C. Gómez de Salazar, A. Sepúlveda-Escribano, F. Rodríguez-Reinoso, Colloids Surf. 187–188 (2001) 151.
[24] S.K. Milonjic, Colloids Surf. 149 (1999) 461.
[25] J. Xie, Q. Zhang, K.T. Chuang, J. Catal. 191 (2000) 86.
[26] T.J. Bandosz, K. Putyera, J. Jagiello, J.A. Schwarz, Microporous Mater. 1 (1993) 73.
[27] J.H. De Boer, The Dynamical Character of Adsorption, Clarendon, Oxford, 1953.
[28] M.A. Montes-Morán, A. Martínez-Alonso, J.M.D. Tascón, Fuel Process. Technol. 77 (2002) 359.
[29] R.A. Bailey, K.C. Persaud, Anal. Chem. Acta 363 (1998) 147.
[30] J.W. Dove, G. Buckton, C. Doherty, Int. J. Pharmcol. 138 (1996) 199.
[31] J. Jagiello, T.J. Bandosz, J.A. Schwarz, J. Colloid Interface Sci. 151 (1992) 433.
[32] A. Van Asten, N. Van Veenendaal, S. Koster, J. Chromatogr. A 888 (2000) 175.
[33] R.C. Weast, Handbook of Chemistry and Physics, 69 ed., CRC Press, USA, 1988.
[34] E. Díaz, S. Ordóñez, A. Vega, J. Coca, Microporous Mesoporous Mater. 70 (2004) 109.
[35] A. Auroux, R. Monaci, E. Rombi, V. Solinas, A. Sorrentino, E. Santacesaria, Thermochim. Acta 379 (2001) 227.